Evaluation of Reversible Screw Compressors with an Adaptable Built-In Volume Ratio in Reversible Heat Pumps

Florian Kaufmann[1]*, Christopher Schifflechner[1], Fabian Dawo[1], Christoph Wieland[1,2], Hartmut Spliethoff[1,3]

[1]Technical University of Munich, Chair of Energy Systems, Garching, Bavaria, Germany

[2]Technical University of Munich, Munich School of Engineering, Garching, Bavaria, Germany

[3]Bavarian Centre for Applied Energy Research, Garching, Bavaria, Germany

*Corresponding Author: florian.k.kaufmann@tum.de

ABSTRACT

Reversible heat pumps consisting of a high-temperature heat pump and an Organic Rankine Cycle have been subject to increasing academic interest in recent years. Early experimental studies suggested the use of separate compression and expansion devices due to different process conditions in both operating modes. While this concept enables higher machine efficiencies, it also drives up the system cost and can make the concept economically unattractive. In recent years, twin-screw compressors with an adaptable built-in volume ratio (BVR) have become available, allowing efficient machine operation over a wider range of operating conditions. Since this type of compressor is inherently reversible (allowing operation as an expander), it should be considered for use in reversible heat pumps with a single compressor/expander unit. This work makes use of a recently developed model for volumetric screw compressors and expanders to evaluate the potential of machines with an adaptable BVR. A reversible heat pump with a single compressor/expander unit is deployed within a geothermal CHP plant model and annual simulations are performed based on the adapted load profiles of an existing district heating plant. The yearly net electricity production is compared for adaptable BVR machines and the more established fixed-BVR machines. For the observed scenario, the yearly net electricity production rises by 3.1 % due to the deployment of adaptable BVR machines

1 INTRODUCTION

Reversible heat pumps (RHPs), combining an Organic Rankine Cycle (ORC) and a high-temperature vapour compression heat pump (HTHP), have become the subject of an increasing number of academic publications. While the ORC technology is widely established in low-temperature heat utilisation (Quoilin *et al.*, 2013) , HTHPs can be deployed to upgrade otherwise unused heat (e.g. industrial waste heat or ambient heat) for further use at higher temperature levels (Arpagaus *et al.*, 2018). Different applications have been proposed for RHPs in literature. Dumont *et al.* (2015) proposed the application in the building sector (e.g. in the context of a Net Zero Energy Building) and also presented a proof-of-concept, constructing a fully reversible experimental RHP facility. In addition, Quoilin *et al.* (2016) confirmed this technology's ability to produce significant amounts of electricity (next to its primary task of space heating) by the means of annual simulations. Kosmadakis and Panagiotis (2019) show the potential for increased profits of RHPs compared to mono-functional plants in an industrial context despite their higher initial cost. Steinmann *et al.* (2019) present various application scenarios for RHPs serving as a sector-coupling technology with the overall goal of decarbonising the heat and electricity supply. In a similar context, Urbanucci *et al.* (2019) highlight the ecological and economic advantages of RHPs compared to conventional (fossil) backup technologies for peak load times. The recently most investigated application of RHPs is their use in pumped thermal electricity storages (PTES). Frate *et al.* (2017) introduce a thermally integrated PTES relying on a RHP and investigate the effect of different

heat source temperatures and working fluids. Staub *et al.* (2018) consider the effect of different process topologies on the roundtrip efficiency of PTES systems. Volumetric compressors, which are frequently used in small to medium scale heat pumps, can be reversed to work as expanders as it has been shown in experimental facilities using Scroll (Dumont *et al.*, 2015) and Twin-Screw compressors (TSC) (Eyerer *et al.*, 2020a). While the reversible operation of piston compressors is also possible, it requires modifications in the valve timing (Dumont, 2017), which makes the reversible operation inherently more complex compared to Scroll and Twin-Screw machines. For this reason, Scroll and Twin-Screw machines are more established when it comes to reversible operation. The aforementioned reversibility intuitively suggests the reversible use of one compression/expansion device in a RHP due to declining plant costs. However, several authors point out that the efficiency of reversibly used volumetric compression/expansion machines significantly decreases in at least one operational mode due to the different process conditions (Frate *et al.*, 2017; Staub *et al.*, 2018; Dumont and Lemort, 2019). A potential solution for this issue is the reversible use of TSCs with an adaptable built-in volume ratio. These can achieve high efficiencies over a wider range of process conditions (e.g. pressure ratios) compared to common volumetric compressors. This work aims at screening the potential of adaptable-BVR machines compared to the established fixed-BVR models. A semi-empiric model for TSCs with an adaptable BVR (recently developed by the authors (Kaufmann *et al.*, 2020)) and a model for fixed-BVR TSCs taken from literature are embedded in simulations of a RHP and compared based on system performance. System performance is evaluated based on annual simulations of a geothermal CHP plant, which in turn rely on realistic load profiles from an existing facility and a typical-day approach described subsequently.

2 MACHINE MODELLING

Evaluating the performance of both fixed-BVR and variable-BVR TSCs (and the respective expanders) within a simulation requires suitable component models. For this work, a semi-empirical modelling approach is chosen due to its numerical stability, fast calculation and extrapolation capability.

2.1 Fixed BVR model

For the fixed-BVR TSCs a model presented in literature (Giuffrida, 2016) is applied. The general model structure is depicted on the left in Figure 1. The suction gas stream $\dot{m}$ is first mixed with the internal leakage stream $\dot{m}_{leak}$ (1→2) and subsequently heated by a heat flux $\dot{Q}_{su}$ from the compressor housing (2→3) which is modelled as a fictitious isothermal envelope. The gas is then compressed up to a pressure determined by the BVR of the machine in an isentropic compression step (3→4). This is followed by an isochoric compression or expansion to the applied head pressure of the machine (4→5), which allows accounting for the effect of over and under-compression. The required internal compression power P_{int} is a central model parameter and can be determined by

$$P_{int} = \dot{m}_s \cdot \left((h_4 - h_3) + v_4 \cdot (p_5 - p_4)\right) \tag{1}$$

including the swept mass flow $\dot{m}_s$, the outlet pressure p_5, the specific enthalpy after suction warming h_3 as well as the pressure p_4, specific enthalpy h_4 and specific volume v_4 after the isentropic compression. The compressed gas subsequently releases the heat flux $\dot{Q}_{ex}$ to the compressor housing (5→6) and is finally split into the leakage stream and the outlet stream. The model includes friction losses (P_{loss}), which are rejected to the compressor housing as friction heat. Moreover, the compressor gives off the heat flux $\dot{Q}_{amb}$ to its surroundings, depending on the ambient temperature and the compressor housing temperature. The model is fully described by eight parameters, of which six must be fitted to operational data of the individual compressor. For the model to be solved, the energy balances around the compressor housing and around the whole compressor must be satisfied. The first is defined as

$$P_{loss} - \dot{Q}_{amb} + \dot{Q}_{ex} - \dot{Q}_{su} = 0 \tag{2}$$

while the latter can be written as

$$P_{sh} - \dot{Q}_{amb} + \dot{m} \cdot (h_6 - h_1) = 0 \tag{3}$$

Apart from the specific inlet and outlet enthalpy (h_1 and h_6) the required shaft power P_{sh}, defined as the sum of the internal compression power and friction losses, is necessary to calculate the energy balance given in equation (3). Since the thermal envelope temperature and the outlet state are not known a priori, they must be determined iteratively by numerical minimisation of the residuals from equations (2) and (3). For further information on the model, the interested reader is referred to the original publication by (Giuffrida, 2016).

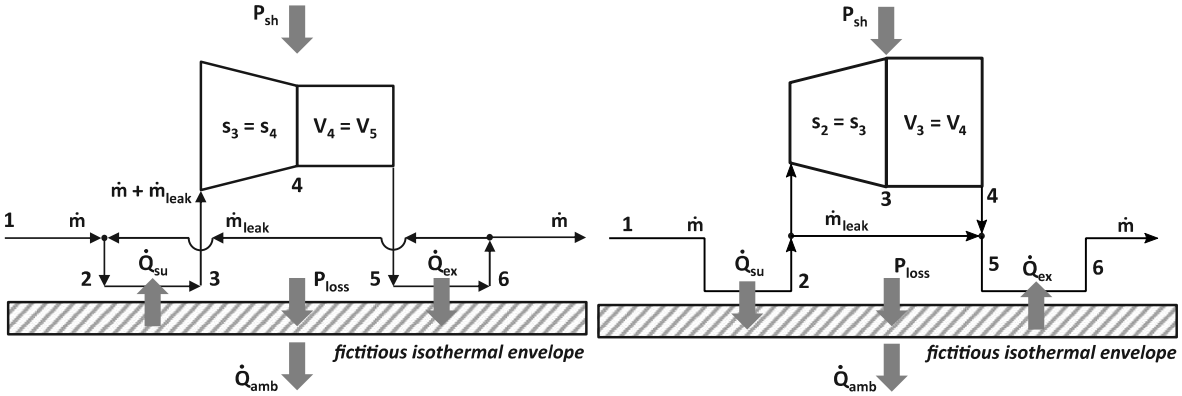

Figure 1: Twin-screw compressor model (left) according to (Giuffrida, 2016) and according expander model (right) for reversible operation

Since TSCs are usually fully reversible, only minor modifications to the above presented model are necessary to simulate the behaviour of a twin-screw expander (TSE). The expander model used in this work is depicted on the right in Figure 1. It shares key process features with the previously described compressor model and hence shares most model parameters. Since the underlying physical processes in the machine do not change significantly, most parameters of the compressor model can be adopted for the expander model when simulating reverse operation of the same machine. Only the model parameters for the internal heat transfer on the suction and exhaust side need to be switched in the expander model to account for the change in flow regime. A TSE model very similar to the one presented above has been developed and experimentally validated for TSEs by Dawo *et al.* (2021).

2.2 Variable BVR model

The compressor with a variable BVR is calculated using a novel model recently developed by the authors (Kaufmann *et al.*, 2020). It is based on the model described in the previous section but can account for a changing BVR and hence shows good machine efficiencies over a wider range of pressure ratios. The BVR can be adapted within the allowed range defined by the input parameters BVR_{min} and BVR_{max} (depending on the specific compressor model). In a first step, the model estimates the ideal BVR (BVR_{id}, which is used as the input for further calculations) from the applied pressure ratio.

$$BVR_{id} = \frac{v_1}{v_{id}} \tag{4}$$

In this equation, v_1 and v_{id} are the specific volumes of the working fluid at the compressor inlet and after an isentropic compression to the specified outlet pressure. If the value of BVR_{id} exceeds the allowed range it is set to the nearest permitted value. After BVR_{id} is identified, the dependent parameter $a_{tl,1}$ (correlating the speed-independent torque losses to the internal compression power) is calculated by a polynomial correlation of the form:

$$a_{tl,1} = a \cdot BVR_{id}{}^{b} + c \tag{5}$$

For pressure ratios resulting in BVR_{id} values outside the allowed range, the value for $a_{tl,1}$ is calculated using BVR_{min} and BVR_{max} respectively. The dimensionless parameters a, b and c are fitted to operational

compressor data together with the remaining model parameters. This results in eleven model parameters of which eight must be fitted to experimental data. In a previous work (Kaufmann et al., 2020), the model was validated for a specific compressor model using operational data provided by the manufacturer showing very high accuracy. The mean deviation between the model outputs and the catalogue data is 0.83 %, 0.52 % and 1.50 % for the shaft power, the outlet temperature and the compressor speed respectively. For the calculation of the variable-BVR TSE, the same assumptions from the previous section are applied and only two model parameters need to be switched.

The variable-BVR compressor observed in this work is a *Bitzer CSW10593* with a BVR adaptable in the range between 1.7 and 3.5 and a swept volume of roughly 11.5 litres. In order to allow for a fair comparison with no initial offset in compressor or expander efficiency, the fixed-BVR machines are simulated using the same model parameters as the variable-BVR model but keeping the BVR value constant.

3 SIMULATION METHODOLOGY

3.1 System description and simulation tools

The performance assessment of the reversible compressor/expander is done by including the previously described compressor and expander models in a RHP operated within a geothermal combined heat and power (CHP) plant. In this system, the primary use of the geothermal brine is to supply heat to a district heating network (DHN). On warm days, when the fixed geothermal heat supply surpasses the DHN heat demand, excess heat is used to run the RHP in ORC mode and produce electricity as depicted in Figure 2a. In contrast, when the DHN heat demand exceeds the geothermal supply on cold days, the RHP runs in the HTHP mode to supply additional heat to the DHN. In this operation mode, the RHP further cools down the geothermal brine after the DHN heat exchanger and heats up the portion of the DHN flow that cannot be heated up by the brine (see Figure 2b).

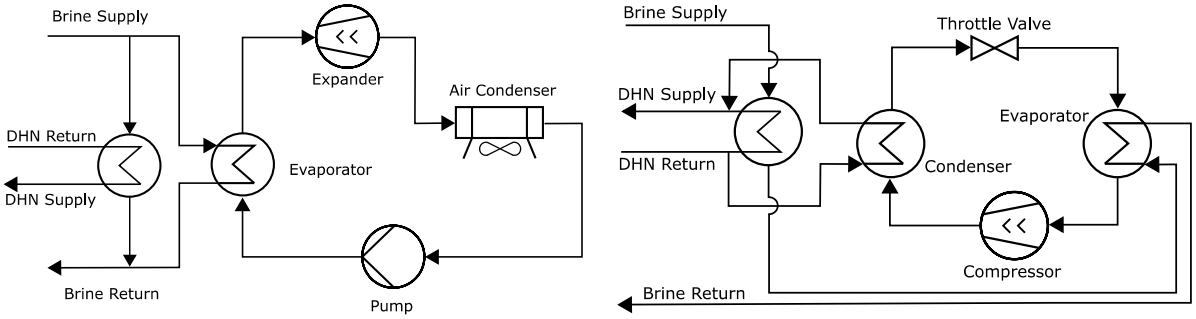

a) b)

Figure 2: ORC mode (a) and HTHP mode (b) for a RHP in a geothermal CHP plant

While the ORC uses an air condenser (due to limited availability of cooling water in practical applications), the HTHP requires an additional heat exchanger to condense against DHN water. The simulation of both operation modes is conducted in the commercial process simulation software *Ebsilon Professional 14*. It allows custom component models to be included that are solved simultaneously with the remaining unit operations of a flowsheet. The component models described in Section 2 were therefore implemented in *Ebsilon Professional 14* in order to simplify the simulations. Table 1 summarises the most important simulation parameters of the RHP for both operation modes. Since a RHP is inherently highly flexible in its operating conditions, the heat exchangers have to be considered with extra care. However, this would extend the scope of this work and the heat exchangers are therefore simulated with fixed heat transfer coefficients.

Table 1: Simulation parameters for ORC and HTHP operation of the RHP

ORC Operation		HTHP Operation	
Evaporating pressure in bar	5.00	Compressor inlet superheating in K	5.00
Expander inlet superheating in K	5.00	Evaporator pinch ΔT in K	5.00
Evaporator pinch ΔT in K	5.00	Condenser pinch ΔT in K	5.00
Condenser pinch ΔT in K	5.00	Brine inlet temperature in °C	60.00
Isentropic pump efficiency	0.80	DHS return temperature in °C	50.00
Electric motor/generator efficiency	0.95	Brine flowrate in kg/s	65.00
Cooling air ΔT in K	10.00		
Brine inlet temperature in °C	118.00		

The brine flow rate in ORC mode and the DHN water flow rate heated by the HTHP are determined by the individual load profiles and will be discussed in Section 3.2 subsequently. The mass flow rate of the ORC working fluid is set by a controller in order to maintain 5 K superheating at the expander entrance for the respective evaporating pressure. For the HTHP, the mass flow rate of the working fluid is also set by a controller in order to supply the required amount of heat for the DHN. Relying on recommendations in literature, R1233zd(E) is used as working fluid in both operation modes.

The evaporating pressure in ORC mode is determined with the goal to achieve the maximum net power output (by cooling down the brine as far as possible). A first screening showed optimal evaporating pressures between 5 and 6 bar, so for the sake of simplicity a value of 5 bar was adopted for all ORC operation points. The ORC condensation pressure is controlled to satisfy the pinch point constraint in the condenser with the minimum allowed pressure being 1.1 bar for practical reasons. In HTHP mode the compressor head pressure is set to the minimum value that does not conflict with the pinch point constraint, thereby minimising the required compressor power. Similarly the evaporation pressure is set to its maximum possible value not conflicting with the evaporator pinch point constraint.

It can be deducted from the previous two paragraphs that a preliminary optimisation of the process conditions is performed for each observed simulation point. Only the evaporating pressure in ORC mode should still be optimised for each individual operating point. However, this is more complex than the previously discussed optimisations and exceeds the scope of this work.

3.2 Typical-day method and load profiles

Annual system simulations with hourly resolution are an effective method for evaluating the performance of different process topologies and machine types under realistic operation conditions. In the context of this work, the method accounts for the variation of important factors such as changing ambient temperatures and heat demands based on seasonal and daily fluctuations. However, the calculation of several thousand operating point comes with a significant effort and automation can be prone to error when numerical instability occurs in some part of the calculation. Hence, this work applies the typical-day approach described in the VDI 4655 guideline (VDI-Gesellschaft Energietechnik, 2008). It introduces ten typical days, which occur with a certain frequency throughout the year depending on the geographical location or climate zone. Since each typical day is represented by a reference load profile (RLP) with an hourly resolution, a total of 240 system states must be calculated in the simulation.

In order to create the RLP for each typical day, this work combines hourly weather data (e.g. ambient temperatures and cloudiness) for the location of Munich with the heat demand profile of an existing geothermal heating plant in the south of Munich, both for the year 2016. Based on the existing data, a slightly adapted hypothetical – but potentially realistic – application scenario is created. It is characterised by a lower geothermal heat supply leading to insufficient DHN heat demand coverage during the winter days and lower available heat for geothermal power generation during the rest of the year. Thus, the application of a flexible and efficient RHP system would be of high interest in such an application case. The frequency of each typical day obtained from the weather data is given in Table 2.

The criteria for the typical day categories (described by a three-letter code, see Table 2) are the daily mean cloudiness and the daily mean temperature. The first letter of the category is either "S" for summer, "W" for winter or "T" for the transitional period. The criteria for each named season are a daily mean temperature larger than 15°C, smaller than 5°C or a value in between respectively. The second letter is either "W" for workdays (including Saturdays) or "S" for Sundays. The third letter accounts for the cloudiness and is "B" for bright days with a mean cloudiness smaller than 5/8 or "C" for cloudy days with a mean cloudiness larger or equal to 5/8. For summer days, the cloudiness has little impact on the daily temperature curve, so it is neglected, and the third letter is simply "X".

Table 2: Frequency of typical days according to VDI 4655 for Munich in 2016

Category:	*SWX*	*SSX*	*WWB*	*WWC*	*WSB*	*WSC*	*TWB*	*TWC*	*TSB*	*TSC*
Category No.:	*1*	*2*	*3*	*4*	*5*	*6*	*7*	*8*	*9*	*10*
Frequency:	100	16	20	66	5	12	40	87	6	13

Figure 3a shows the sorted yearly DHN heat demand based on the scaled data from the existing plant. The available geothermal heat supply can cover the demand for 6804 hours while the HTHP must supply additional heat for 1956 hours per year.

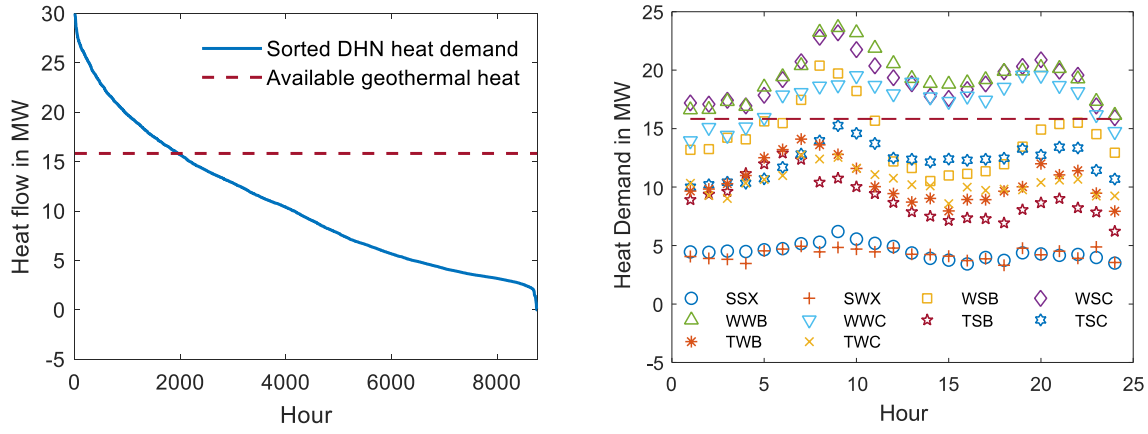

a) b)

Figure 3: Sorted yearly heat demand (a) and hourly heat demand of all typical day RLPs (b) with the available geothermal heat indicated by the dashed red line in subfigure (b)

In order to determine the RLP for ambient temperature, DHN heat demand and DHN supply temperature for each typical day, the mean value of each parameter (in form of a mean 24-hour profile) is calculated over all days within each category.

Using the mean profile, the root mean square error (RMSE) of each parameter is calculated for all days within each category and the profile with the smallest RMSE is set as the RLP for the respective parameter of each category. As an example, Figure 3b shows the hourly heat demand RLP of each typical day category generated from the available data. It can be observed that the HTHP must be operated at least for a few hours on every typical winter day while the ORC can be operated every day in the summer and transitional season. The RLPs in Figure 3b result in 2042 hours of HTHP operation while the ORC can be operated 6718 hours per year. This shows that the deviation from the actual heat demand profile from Figure 3a is reasonably small and the reduction in simulation time and complexity generally outweighs the loss in accuracy.

Both compressor types are compared based on the yearly net electricity production E_{net}, which can be calculated by subtracting the HTHP's yearly electricity use E_{HTHP} from the ORC's net electricity generation $E_{\mathrm{net,ORC}}$.

$$E_{\text{net}} = E_{\text{net,ORC}} - E_{\text{HTHP}} \tag{6}$$

The latter is calculated by subtracting the electricity use of the pump E_{pump} and the air condenser E_{cond} from the gross electric power $E_{\text{gross,ORC}}$ generated by the ORC. It must be noted that the electrical demand for the geothermal brine pump is not considered since its electrical power demand depends on the actual local geological conditions of a geothermal project.

$$E_{\text{net,ORC}} = E_{\text{gross,ORC}} - E_{\text{pump}} - E_{\text{cond}} \tag{7}$$

E_{HTHP} (in MWh) is calculated from the electrical compressor power $P_{\text{el,HTHP},i,j}$ (in MW) of each state within the ten typical day categories and the frequency of each typical day $n_{\text{typical day},i}$ taken from Table 2. Here $P_{\text{el,HTHP},i,j}$ is set to zero for all RLP points without HTHP operation.

$$E_{\text{HTHP}} = \sum_{i=1}^{10} \left(\sum_{j=1}^{24} P_{\text{el,HTHP},i,j} \cdot 1\text{h} \right) \cdot n_{\text{typical day},i} \tag{8}$$

$E_{\text{net,ORC}}$ is obtained by replacing $P_{\text{el,HTHP},i,j}$ in Equation (8) with the electrical net power $P_{\text{el,net,ORC}}$ (in MW) of the ORC. Similar to the calculation of E_{HTHP}, the ORC net power is set to zero for all RLP points without ORC operation.

4 RESULTS AND DISCUSSION

The RLPs described in Section 3.2 are first simulated for the reversible machine with variable BVR. In order to ensure a fair comparison for the fixed-BVR machine, the ideal BVR is determined from the results for variable-BVR operation. For this, the weighted mean BVR is calculated for both operation modes by multiplying the actual BVR of all valid operation points with the number of their occurrences throughout the year and summing them up before dividing the sum by the total number of yearly operating hours of the respective operating mode. The weighted mean BVR of both operation modes is then combined by multiplying each value with the operating mode's fraction of total operating hours and summing up the results. With a mean weighted BVR of 2.42 for HTHP operation and 3.19 for ORC operation respectively, the ideal fixed BVR turns out to be 3.0. The most important results for both machine models are summarised in Table 3 and Table 4.

Table 3: Isentropic compressor and expander efficiency for variable and fixed BVR

	Variable BVR		BVR = 3.0	
	ORC	HTHP	ORC	HTHP
$\eta_{\text{is,min}}$ in %	75.37	73.27	73.60	69.71
$\eta_{\text{is,max}}$ in %	78.18	80.38	77.82	80.35
$\eta_{\text{is,mean}}$ in %	77.57	78.75	76.29	77.29

As expected, both operating modes perform better with the variable-BVR machine, since the compressor and expander can adapt better to changing operating conditions. Table 3 indicates that the maximum compressor and expander efficiency remains roughly constant independent of the BVR. The minimum machine efficiency as well as the mean machine efficiency decreases for the fixed-BVR machines. This is caused by the more distinct effect of over and under-compression/expansion in the fixed-BVR machines. Compared to the fixed-BVR operation, the yearly electricity use of the HTHP declines by 1.2 % while the net electricity production of the ORC rises by 2 % due to the variable BVR. This adds up to a 3.1 % (or 51 MWh) rise in the yearly net electricity production of the system due to the variable-BVR machine. To give an idea of the potential economic benefits, a more detailed analysis based on the German electricity market is conducted. It accounts for the mismatch between feed-in

tariffs of 25.2 ct/kWh and purchase prices around 13 ct/kWh for ORC plant operators (Eyerer *et al.*, 2020b).

Table 4: Yearly electricity use and production with variable and fixed BVR

Var. BVR		BVR = 3.0	
E_{HTHP} in MWh	840	E_{HTHP} in MWh	850
$E_{\mathrm{net,ORC}}$ in MWh	2534	$E_{\mathrm{net,ORC}}$ in MWh	2493
E_{net} in MWh	1694	E_{net} in MWh	1643

The increased performance of the variable-BVR machines would result in additional yearly revenues of 11,762 €. As a general trend, a variable BVR is becoming state of the art for commercial mid- to large-capacity TSCs and hence the price difference between fixed-BVR and variable-BVR machines can be expected to decline, if not disappear. The surplus cost for a variable-BVR machine could hence be covered within a rather short timeframe by the additional revenue generated by the variable BVR.

It should be noted that the presented scenario may not be optimal for assessing the full potential of variable-BVR machines in RHPs. While the variable BVR of the considered compressor model is utilised to nearly its full extent in HTHP mode (BVR from 1.84 to 3.5), the ORC (BVR from 2.28 to 3.5) uses only a smaller fraction of the available BVR range (1.7 to 3.5) due to larger pressure ratios. This also manifests itself in the mean weighted BVR value for both operation modes as presented above. This calls for further comparison of both machine types within different scenarios, e.g. for different climate zones, lower wellhead temperatures or PTES applications using different heat sources and storage temperatures.

The volatile heat demand in the DHS network results in a strong variation of the working fluid flow rate for both operation modes (i.e. 0.59 kg/s to 42.55 kg/s in HTHP mode and 2.55 kg/s to 55.77 kg/s in ORC mode) . However, since twin-screw machines are usually able to cover a wide speed range, this poses no major obstacle. In ORC mode only one operating state results in an expander speed lower than 1000 rpm (i.e. 883 rpm), which is at the lower end of typical operating speeds for TSEs. In HTHP mode four operating states exhibit a compressor speed lower than 1000 rpm. Assuming a minimum compressor compressor/expander speed of 1000 rpm, this would result in a reduction of 95 yearly operating hours in HTHP mode and 20 yearly operating hours in ORC mode respectively. Since the compressor and expander power at these low rotational speeds is very low compared to most other operating points, the impact on the overall system performance is only minor. The higher working fluid flow rates are a more severe problem, leading to unrealistially high machine speeds in a single compressor or expander. However, it is possible to operate several machines in parallel to handle larger flow rates, which would also enhance plant flexibilty. In this context, piping and heat exchangers also have to be considered with special care to avoid high pressure losses and insufficient heat transfer. Similar to the compressor, this issue can be tackled by operating several heat exchangers in parallel according to the momentary system requirements. Since the main focus of this work is the effect of varying pressure ratios on the machine efficiency, the flow rate will not be further discussed.

Independent of the effect of the variable BVR, the RHP supplies a total heat of 5650 MWh to the DHN during HTHP operation. This would have to be covered either by a large seasonal storage system or by fossil support firing in a regular geothermal heating plant, with the latter being to currently more common application solution. Considering the current stock exchange price of roughly 8.3 €/MWh for natural gas this would result in yearly surplus cost of 46,895 € for fossil firing in the given scenario.

5 CONCLUSIONS

This work evaluates the potential benefits of variable-BVR twin-screw machines as reversible compressor/expander units in reversible heat pumps. Their performance is compared to the widely established fixed-BVR machines by means of annual simulations for a reversible heat pump system operated within a geothermal CHP plant. The simulated plant trajectory is based on real plant and weather data for a geothermal heating plant outside Munich (Germany) and uses a typical day method to reduce the number of plant states to be calculated. The typical day approach significantly reduces the computational effort while still being reasonably accurate with respect to the initial plant load profile. Both machine types and their reaction to changing operation conditions are accounted for by including detailed semi-empiric component models into the simulation. The variable-BVR machine shows a promising improvement of the plant performance with a 3.1 % increase of the plant's yearly net electricity production. The positive impact of the variable-BVR machine needs to be validated for different operation scenarios in future work using the previously presented framework. Special focus will be a more extensive utilisation of the full variable BVR range in ORC mode, for example by operation in warmer climate or by the use of geothermal brine with lower wellhead temperatures. In addition, the application in PTES systems will be evaluated. The numbers for the increased revenue due to the variable BVR and the saved expanses for fossil support firing are a good indicator for the high potential of reversible heat pumps in geothermal CHP plants. However, they should be considered carefully until a more detailed techno-economic analysis of the plant has been conducted to provide more substantive numbers.

NOMENCLATURE

Symbols

E	Electrical energy	(MWh)
h	Specific enthalpy	(J/kg)
$\dot{m}$	Mass flow	(kg/s)
n	Number	(-)
p	Pressure	(Pa)
P	Power	(W)
$\dot{Q}$	Heat flow	(W)
v	Specific volume	(m³/kg)

Subscripts

amb	Ambient
cond	Air condenser
ex	Exhaust
el	electrical
id	Ideal
int	Internal
s	Swept
su	Suction
tl	Torque loss

Abbreviations

BVR	Built-in volume ratio
CHP	Combined heat and power
DHN	District heating network
HTHP	High temperature heat pump
ORC	Organic Rankine cycle
RHP	Reversible heat pump
RLP	Reference load profile
RMSE	Root mean square error
TSC	Twin-screw compressor
TSE	Twin-screw expander

ACKNOWLEDGEMENT

Funding from the Bavarian State Ministry of Education, Science and the Arts in the framework of the project Geothermal-Alliance Bavaria is gratefully acknowledged.

6 References

Arpagaus, C., F. Bless, M. Uhlmann, J. Schiffmann, and S. S. Bertsch, 2018, "High temperature heat pumps: Market overview, state of the art, research status, refrigerants, and application potentials", Energy **152**, 985.

Dawo, F., S. Eyerer, R. Pili, C. Wieland, and H. Spliethoff, 2021, "Experimental investigation, model validation and application of twin-screw expanders with different built-in volume ratios", Applied Energy **282**, 116139.

Dumont, O., 2017, "Investigation of a heat pump reversible in an organic Rankine cycle and its application in the building sector", PhD Thesis (University of Liège).

Dumont, O., and V. Lemort, 2019, "Thermo-technical approach to characterize the performance of a reversible heat pump/organic Rankine cycle power system depending on its operational conditions", Proceedings of ECOS 2019.

Dumont, O., S. Quoilin, and V. Lemort, 2015, "Experimental investigation of a reversible heat pump/organic Rankine cycle unit designed to be coupled with a passive house to get a Net Zero Energy Building", International Journal of Refrigeration **54**, 190.

Eyerer, S., F. Dawo, C. Wieland, and H. Spliethoff, 2020a, "Advanced ORC architecture for geothermal combined heat and power generation", Energy **205**, 117967.

Eyerer, S., C. Schifflechner, S. Hofbauer, W. Bauer, C. Wieland, and H. Spliethoff, 2020b, "Combined heat and power from hydrothermal geothermal resources in Germany: An assessment of the potential", Renewable and Sustainable Energy Reviews **120**, 109661.

Frate, G. F., M. Antonelli, and U. Desideri, 2017, "A novel Pumped Thermal Electricity Storage (PTES) system with thermal integration", Applied Thermal Engineering **121**, 1051.

Giuffrida, A., 2016, "A semi-empirical method for assessing the performance of an open-drive screw refrigeration compressor", Applied Thermal Engineering **93**, 813.

Kaufmann, F., C. Wieland, and H. Spliethoff, 2020, "Validation of a Semi-Empiric Model for Twin-Screw Compressors with an Adaptable Internal Volume Ratio", Proceedings of the 12th International Conference on Applied Energy. Part1.

Kosmadakis, G., and N. Panagiotis, 2019, "POTENTIAL AND COST EFFECTIVENESS OF A REVERSIBLE HIGH-TEMPERATURE HEAT PUMP/ORC UNIT FOR THE EXPLOITATION OF INDUSTRIAL WASTE HEAT", Proceedings of the 5th International Seminar on ORC Power Systems.

Quoilin, S., O. Dumont, K. Harley Hansen, and V. Lemort, 2016, "Design, Modeling, and Performance Optimization of a Reversible Heat Pump/Organic Rankine Cycle System for Domestic Application", Journal of Engineering for Gas Turbines and Power **138**.

Quoilin, S., M. van den Broek, S. Declaye, P. Dewallef, and V. Lemort, 2013, "Techno-economic survey of Organic Rankine Cycle (ORC) systems", Renewable and Sustainable Energy Reviews **22**, 168.

Staub, S., P. Bazan, K. Braimakis, D. Müller, C. Regensburger, D. Scharrer, B. Schmitt, D. Steger, R. German, S. Karellas*, et al.*, 2018, "Reversible Heat Pump–Organic Rankine Cycle Systems for the Storage of Renewable Electricity", Energies **11**, 1352.

Steinmann, W.-D., D. Bauer, H. Jockenhöfer, and M. Johnson, 2019, "Pumped thermal energy storage (PTES) as smart sector-coupling technology for heat and electricity", Energy **183**, 185.

Urbanucci, L., D. Testi, and J. C. Bruno, 2019, "Integration of Reversible Heat Pumps in Trigeneration Systems for Low-Temperature Renewable District Heating and Cooling Microgrids", Applied Sciences **9**.

VDI-Gesellschaft Energietechnik, 2008, "Referenzlastprofile von Ein- und Referenzlastprofile von Ein- und Mehrfamilienhäusern für den Einsatz von KWK-Anlagen".